Virology 603 (2025) 110360

Contents lists available at ScienceDirect

Virology

journal homepage: www.elsevier.com/locate/virology

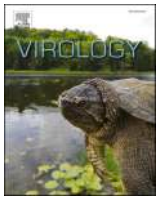

Comparative analyses of three grapevine Pinot gris virus cDNA clones reveal insights into the pathological properties of different phylogroups

Dipendra Karki [a,*], Rita Musetti [b,c], Baozhong Meng [a,**]

[a] Department of Molecular and Cellular Biology, University of Guelph, Guelph, Ontario, Canada
[b] Department of Agriculture, Food, Environmental and Animal Sciences, University of Udine, Udine, Italy
[c] Department of Land, Environment, Agriculture and Forestry, University of Padua, Viale dell' Universita, 16 – Agripolis, 35020, Legnaro (PD), Italy

ARTICLE INFO

Handling Editor: Prof. Xue-Ping Zhou

Keywords:
Grapevine
GPGV
GLMD
Phylogenetic analysis
RT-PCR
RT-qPCR
Infectious clone
Virus titre
Yield

ABSTRACT

Grapevine Pinot gris virus (GPGV) is an emerging grapevine virus associated with grapevine leaf mottling and deformation (GLMD) disease. Being a recently identified virus, the molecular biology, pathological properties, and etiological complexity of GPGV remain poorly studied. Previous research revealed that GPGV comprises genetically different variants, some encoding a larger movement protein (MP) and others a shorter MP due to a C/T polymorphic site in ORF2 encoding MP. Variants that encode the shorter MP are associated with severe disease, whereas variants encoding the longer MP are associated with mild or no symptoms. However, this has yet to be demonstrated experimentally. Here, we report the construction of a wildtype cDNA clone, pGPGV-SY, based on ON93-12, a local isolate from Syrah closely related to the variants encoding the larger MP. Surprisingly, our clone exhibited significantly faster replication and caused more severe disease symptoms than pRI::GPGV-lat, an Italian GPGV clone, with a longer MP and demonstrated similar efficacies with that of pRI::GPGV-vir, another Italian clone with a shorter MP. A single C to T mutation at the polymorphic site of pGPGV-SY resulted in a two-fold higher RNA accumulation in the grapevine. Findings from this work constitute a leap toward the long-standing and complex question pertaining to the relationship between GPGV variant groups and GLMD. Integrating findings from this work and those by others, we propose an updated model to explain the complex relationship between GPGV variants and GLMD.

1. Introduction

Viticulture recently faced an emerging grapevine virus, grapevine Pinot gris virus (GPGV; *Trichovirus pinovitis*), associated with the grapevine leaf mottling and deformation disease (GLMD) (Cieniewicz et al., 2020; Giampetruzzi et al., 2012; Saldarelli et al., 2015; Tarquini et al., 2023). GPGV is a member of the genus *Trichovirus* within the family *Betaflexiviridae* and has a positive sense, single-stranded RNA molecule of 7259 nucleotides (nt) plus a poly(A) tail with three overlapping open reading frames (ORFs) that encode a replicase protein, movement protein (MP), and coat protein (CP) in the 5′ to 3′ direction (Glasa et al., 2015; Saldarelli et al., 2017). The replicase protein contains methyltransferase, helicase, and RNA-dependent RNA polymerase (RdRp) domains and an alkylation B (AlkB) domain, which is present in a subset of positive-strand, single-stranded RNA viruses infecting perennial plants, most of which are woody perennials (Aravind and Koonin, 2001; Moore and Meng, 2019). The function of viral AlkB in the replication of these viruses is not known, though it was hypothesized to protect viral RNAs from methylation damage (van den Born et al., 2008). The MP plays a critical role in the cell-to-cell movement of viruses through plasmodesmata in the host plant after infection (Lucas, 2006). Besides its role in virion assembly and long-distance movement via the phloem, GPGV CP was shown recently to suppress RNA silencing (Tarquini et al., 2021b).

GPGV was first identified in Trentino, Northern Italy (Giampetruzzi et al., 2012) and now is reported in all grape-growing regions of the world (Cieniewicz et al., 2020; Hily et al., 2021; Saldarelli et al., 2017; Tarquini et al., 2023). In Canada, GPGV is detected in all four provinces where grapevines are grown, but the prevalence in Ontario is highest, reaching up to 34.3% (Vu et al., 2023; Xiao et al., 2018). The global and regional spread of GPGV is enabled by dissemination and clonal propagation of virus-infected plant materials (Fajardo et al., 2017; Messmer

* Corresponding author.
** Corresponding author.
E-mail addresses: dkarki@uoguelph.ca (D. Karki), bmeng@uoguelph.ca (B. Meng).

https://doi.org/10.1016/j.virol.2024.110360
Received 17 October 2024; Received in revised form 5 December 2024; Accepted 11 December 2024
Available online 15 December 2024

et al., 2023; Saldarelli et al., 2015), whereas local spread is via grafting and transmission by grape erineum mites *Colomerus vitis* (*Acari: Eriophyidae*) (Bertazzon et al., 2020; Hily et al., 2020; Malagnini et al., 2016). GPGV has also been detected in non-Vitis hosts, including herbaceous species (Silene latifolia, *Chenopodium album*) and perennials (Ailanthus sp., Asclepias sp., Crataegus sp., Fraxinus sp., Rosa sp., Rubus sp., and Sambucus sp.), which probably serve as a reservoir for its transmission (Demian et al., 2022; Gualandri et al., 2017).

GPGV has been associated with GLMD disease (Giampetruzzi et al., 2012; Saldarelli et al., 2017). However, the type and severity of disease symptoms vary widely depending on grapevine cultivar, GPGV variants involved, and environmental conditions. Leaf mottling and deformation are the most characteristic symptoms of GPGV infections. (Bertazzon et al., 2017; Giampetruzzi et al., 2012). The other symptoms include delayed budburst, shortened internodes, poor shoot growth, bushy growth, reduced vigour, shoot tip necrosis and even vine death (Bertazzon et al., 2017; Kaur et al., 2023; Saldarelli et al., 2015; Tarquini et al., 2021a, 2023). Infected grapevines also exhibited poor fruit sets and delayed and uneven fruit ripening, resulting in reduced yield and quality (Angelini et al., 2015; Bertazzon et al., 2017).

To understand the genetic diversity of GPGV and possible pathological differences that may exist among genetic variants of GPGV, several research groups carried out genetic diversity analyses (Bertazzon et al., 2017; Hily et al., 2021; Kaur et al., 2023; Saldarelli et al., 2015). For the first time, Saldarelli et al. (2015) provided the genetic variability of a few GPGV isolates to demonstrate the existence of two lineages, S and A, which comprised grapevine isolates obtained from symptomatic and asymptomatic sources. The further distinction between these two lineages involved the 375 amino acids long MP encoded by ORF2 of the members of lineage A. In contrast, the MP size was reduced by six amino acids among the members of lineage S, which resulted due to C to T mutation at genomic position 6684 of their genome sequences. Based on these observations, the authors hypothesized that this C/T polymorphism may determine the pathogenicity of GPGV variants. This study was extended by Bertazzon et al. (2017), who analyzed additional GPGV isolates, which led to the recognition of clades A, B, and C in which clades A and C correlated with the A and S lineages from Saldarelli et al. (2015). In contrast, clade B consisted of isolates collected from the grapevine with no or only mild symptoms. More recently, phylogenetic analyses using partial or complete genome sequences support grouping GPGV variants into four clades (Vu et al., 2023), where clades 1 and 2 correspond to clade A, and clade 3 corresponds to clade B. In contrast, clade 4 is the equivalent of clade C of the three-clade classification Bertazzon et al. (2017). However, it remains unknown if GPGV variants, more closely related to genome sequences, would behave similarly regarding disease phenotype and symptom severity.

A hallmark of GPGV infection is that the severity of symptoms follows a seasonal trend: disease symptoms are most pronounced at the beginning of a growing season, gradually fade as the season progresses, and could disappear entirely later (Angelini et al., 2015; Bertazzon et al., 2017; Tarquini et al., 2019). In line with the seasonality in symptomatology, the titre of GPGV is highest early in the season, declines gradually, and reaches the lowest point at the end of the season (Angelini et al., 2015; Bertazzon et al., 2017; Bianchi et al., 2015). On the other hand, it was suggested that GPGV titre might be correlated with the disease phenotype (Bertazzon et al., 2017; Bianchi et al., 2015), which was supported by infectivity assays in grapevine and *Nicotiana benthamiana* that were infected with full-length cDNA clones representing two lineages of GPGV isolates (Tarquini et al., 2019). The grapevines infiltrated with pRI::GPGV-vir developed symptoms faster, which were more severe and took longer to recover than those inoculated with pRI::GPGV-lat. Further, infection with pRI::GPGV-vir accumulated much higher viral RNA than those infiltrated with pRI::GPGV-lat (Tarquini et al., 2019). We initiated this research to address three objectives: i) to understand the genetic diversity of GPGV in Ontario; ii) to construct a full-length cDNA clone representing Ontario isolates and test its pathological attributes in comparison with the two other GPGV clones reported in the literature; and iii) to study the effects of a single nucleotide mutation at the C/T polymorphic site within MP on the virulence of GPGV and associated symptom severity. We reveal that all GPGV isolates from Ontario belong to either clades 1 or 2. Surprisingly, our GPGV clone behaved more like pRI: GPGV-vir regarding RNA accumulation and disease phenotype. We further demonstrated that the C/T polymorphic site plays an essential role in virulence. These results refute the long-held notion that only GPGV variants of clade C containing shorter MP induce severe GLMD. We present a model to account for the pathogenesis of GLMD involving complex interplay among GPGV genotype, the grapevine host, and environmental factors.

2. Materials and methods

2.1. Grapevine samples for genetic diversity analysis

Grapevine samples used in this study for genetic diversity analysis were a subset of the samples collected during large-scale surveys for grapevine viruses among commercial vineyards in Ontario (Xiao et al., 2018; Xiao et al., 2018). To reflect GPGV diversity in different types of grapes, eight cultivars of *Vitis vinifera* wine grapes (Cabernet sauvignon, Merlot, Cabernet franc, Gamay, Pinot noir, Syrah, Riesling, Pinot gris), nine cultivars of French-American hybrid wine grapes (Baco, Vidal, Concord, Marquette, De Chaunac, Seyval blanc, Chambourcin, Marechal Foch, Frontenac blanc), one North American juice grape cultivars (Niagara), and a table grape (Sovereign Coronation) were collected from several commercial vineyards in Ontario and included in the phylogenetic analysis (Table S1). In addition, two wild grape samples that tested positive for GPGV were included. Each composite sample used for RNA isolation included two leaves, each from five adjacent vines.

2.2. Total RNA isolation

Total RNA was isolated from 50 mg of grapevine leaf tissue using the optimized protocol described by Xiao et al. (2015). The concentration and quality of the isolated RNA were determined with a NanoDrop spectrophotometer (ND-1000, Thermo Fisher Scientific). The integrity of the RNA preps was assessed by gel electrophoresis followed by staining with ethidium bromide (Tarquini et al., 2019).

2.3. RT-PCR, cloning, sequencing, and phylogenetic analysis

First-strand cDNA was prepared with primers specific to GPGV or GAPDH (Glyceraldehyde-3-phosphate dehydrogenase) as a plant reference gene (Bertazzon et al., 2017; Tarquini et al., 2019) using 2 μg of total RNA and the High-Capacity Reverse Transcription Kit (Thermo Fisher) according to manufacturer's instructions. The MP/CP region of GPGV was amplified with primers GPGV6502F and GPGV7152 (Table S3), which produced a 651 bp long amplicon encompassing 204 nt at the 3′ end of the MP gene and most of the CP gene except the last 25 nt. The rationale for choosing this MP-CP region was to include the segment of the MP containing the potential C/T polymorphic site and most of the CP gene, which was the target region for phylogenetic analysis for GPGV among researchers (Bertazzon et al., 2017; Kaur et al., 2023; Saldarelli et al., 2015). These primers were designed to be broad-spectrum based on the consensus sequence of GPGV sequences available in GenBank. RT-PCR products were gel-purified and cloned into a T/A cloning vector generated in our lab, based on Holton and Graham (1991), and transformed into *E. coli* strain JM109. Colony PCR with the same primers was used to identify recombinant plasmids, which were verified through restriction digestion. Five clones from each of the 21 GPGV isolates were sequenced, and distinct sequences were selected from each isolate and used for phylogenetic analysis using MEGA11 (Tamura et al., 2021). Phylogenetic trees were constructed using Maximum Likelihood with 1000 bootstrap iterations (Felsenstein,

1985), available in MEGA11 (Tamura et al., 2021), on the nucleotide sequences of recombinant plasmids derived from PCR amplification of the target region plus the corresponding regions from 16 representative genomes retrieved from GenBank for phylogeny of MP-CP region and or based on complete genome sequences retrieved from GenBank, including isolate ON93-12, which was sequenced in this study, for the phylogeny of genome sequences.

2.4. Generation of full-length infectious cDNA clones of GPGV

A GPGV isolate ON93-12 from the Syrah cultivar was chosen as a source for constructing a full-length cDNA clone. The strategy and the key steps used for the construction of the full-length cDNA clone and its variants are depicted in Fig. 1. To facilitate cloning, the GPGV genome was divided into four fragments (A, B, C, and D) based on the positions of unique restriction sites available or introduced in the genome sequence (Fig. 1A). Four pairs of primers were designed to amplify these fragments (Table S3) with high-fidelity polymerase PaCeR (GeneBio Systems, Toronto, Canada) as described (Goetz et al., 2022). These fragments were purified, cloned into pJET1.2/blunt (Thermo Fisher) and confirmed by restriction digest analysis and sequencing. The four fragments were released from pJET1.2/blunt via restriction digestion and sequentially subcloned into pBlueScript KS. The 35S promoter from cauliflower mosaic virus (CaMV; *Caulimovirus tessellobrassicae*) was amplified from the PHST40 vector sequence (Meng et al., 2013) using primers NotI35S-F and XbaI35S-R (Table S3) and subcloned at the 5' end of GPGV cDNA using Not I and XbaI. The ribozyme sequence of hepatitis delta virus (HDV) plus the transcription terminator of the nopaline synthase gene (Nos) amplified from the same template used for 35S promoter using primers SpeIHDVnosF and SpeInosR (Table S3), which was inserted at its 3′ end using Spe I to ensure the generation of viral RNA with an authentic terminus. Subsequently, the non-viral sequence introduced at the 5′ end of GPGV cDNA by Xba I was removed via SDM using primers GPGVmuXbF and GPGVmuXbR (Table S3). The resulting plasmid containing the full-length cDNA copy of GPGV-SY in pBlueScript KS was designated pBS-GPGV-SY. After removing the upstream Spe I site in GPGV cDNA, the whole cassette containing the 35S promoter, the full-length cDNA copy of GPGV-SY and Nos terminator/HDV ribozyme site was excised through restriction digest with NotI and SpeI and subcloned into a derivative of the binary vector pCB301 (Xiang et al., 1999) for agroinfiltration. The wildtype GPGV-SY clone in the binary vector was designated pGPGV-SY (Fig. 1A).

The mutant clone, pGPGV-SY-C/T (Fig. 1B), was generated through SDM using primers GPGmuC-TF and GPGmuC-TR (Table S3) following the protocol described by Xia and Xun (2017).

2.5. Agrobacterium culture, plant growth, agroinfiltration of Nicotiana benthamiana

The binary vectors containing the wildtype and mutant GPGV clones were mobilized into *Agrobacterium tumefaciens* strain EHA105, described by Weigel and Glazebrook (2006). Agrobacterial cell suspension of

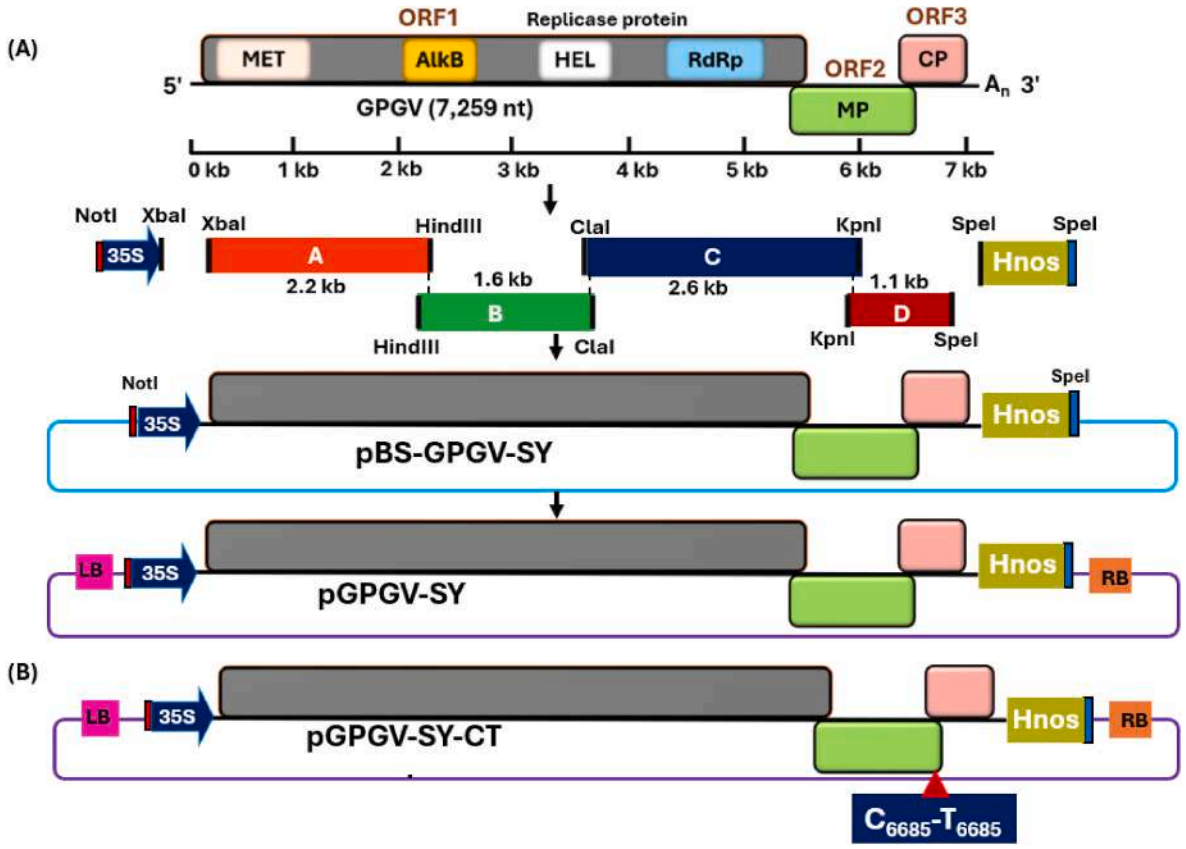

Fig. 1. Diagrammatic representation of the construction of full-length infectious clones of GPGV. **A:** The genome of GPGV contains three open reading frames to encode replicase protein (ORF1), movement protein (ORF2, MP) and coat protein (ORF3, CP). Sequences in the replicase coding sequence corresponding to methyltransferase (Met), Alkylation B (AlkB), helicase (Hel), and RNA Dependent RNA polymerase (RdRp) domains are indicated. The GPGV-SY genome was divided into four fragments, A, B, C, and D, and amplified with a pair of primers each, containing a unique restriction site to generate amplicons of 2209, 1635, 2633, and 1059 bp, respectively. These four fragments, along with the promoter for 35S RNA of cauliflower mosaic virus (35S), hepatitis delta virus ribozyme and nopaline synthase terminator (Hnos), were first cloned into pBluescript KS to generate pBS-GPGV-SY. The restriction enzymes used to subclone these individual fragments are demonstrated. The whole cassette flanked by NotI and SpeI in pBS-GPGV-SY was subcloned into pCB301.3 between the left border (LB) and the right border (RB) to result in pGPGV-SY. **B:** pGPGV-SY-C/T, a C to T mutant clone of GPGV generated by site-directed mutagenesis of wildtype clone of pGPGV-SY.

GPGV clones was prepared as described (Shabanian et al., 2023). Agrobacterium cell suspensions were kept at room temperature in the dark for 3 h to induce the expression of virulence genes (Liu et al., 2019). Where indicated, Agrobacterium containing a plasmid expressing the RNA silencing suppressor (RSS) p19 of tomato bushy stunt virus (TBSV; *Tombusvirus lycopersici*) (Park et al., 2004; Várallyay et al., 2014) was infiltrated with GPGV clones to investigate whether GPGV clones could enhance the infection. The final OD of the Agrobacterium suspension for GPGV clones was adjusted to $OD_{600} = 0.8$ and that of p19 to $OD_{600} = 0.2$. An *Agrobacterium* containing pCB301.3, the empty vector, was used as a negative control.

N. benthamiana plants were grown in growth chambers and infiltrated using a 1-mL needleless syringe on the abaxial side of two to three fully expanded leaves. This was followed by the maintenance of their growth as described (Prudhomme et al., 2024). Infiltrated plants were monitored for symptom development every other day for three weeks. Upper, non-inoculated leaves were subjected to RT-PCR to detect systemic movement of GPGV.

2.6. Agroinfiltration of grapevine plantlets derived from tissue culture

Cabernet franc and Syrah Plantlets were maintained in a growth chamber in the Phytotron at the University of Guelph, essentially as described (Melyan et al., 2015; Shabanian et al., 2023). Foundation Plant Services provided these certified clean stock grapevine materials at the University of California, where mother plants were subjected to meristem tissue culture and tested free of all major viruses, including GPGV. These plants were ensured free of major grapevine viruses, including GPGV, through high-throughput sequencing (HTS) using the Illumina platform, which was conducted as mentioned (Xiao et al., 2019). Furthermore, multiplex RT-PCR was conducted to target 17 major grapevine viruses, including GPGV, using the protocol mentioned (Xiao et al., 2018), which showed the absence of all these major grapevine viruses. The agrobacterial suspension containing GPGV clones and p19, an RNA silencing suppressor (RSS) from TBSV, were prepared as described (Kurth et al., 2012; Shabanian et al., 2023). A final $OD_{600} = 2$ was set for agrobacterial cells containing a GPGV clone, and $OD_{600} = 0.5$ was set for p19 (Kurth et al., 2012). Ten to fourteen-week-old micro-propagated grapevine plantlets were infiltrated with each GPGV clone in combination with an RSS using the optimized vacuum-mediated infiltration method described by (Shabanian et al., 2023). For each GPGV clone, 37 plantlets were agroinfiltrated. The recovery, subsequent growth, and monitoring of the infiltrated plants were conducted essentially as mentioned (Shabanian et al., 2023). Leaf samples were taken from infiltrated plants at multiple intervals and subjected to RT-PCR and RT-qPCR analyses to test infection status and assay viral RNA levels.

2.7. Infectivity assays of GPGV in N. benthamiana and grapevine

The infectivity of the GPGV clones was first examined by RT-PCR with GPGV6502F and GPGV7152R (Table S3) using total RNA extracts. Samples that tested negative with a single round PCR were subjected to nested PCR with GPGV6502F and GPGV7224R. The expected amplification product for the first round PCR is 723 bp, and 651 bp is expected for the second round PCR. GPGV RNA was quantified by RT-qPCR using primers GPGV-504F and GPGV-588R (Table S3) that target an 85 bp sequence of the CP gene. GAPDH was chosen as the reference gene for normalization. GAPDH transcript was demonstrated as the most stable during GPGV infection and thus suitable for the quantification of GPGV by various researchers (Bertazzon et al., 2017; Bianchi et al., 2015; Tarquini et al., 2019). For grape, GAPDH RNA was amplified with VvGAPDH-F and VvGAPDH-R to generate an 80 bp long amplicon, and for *N. benthamiana* GAPDH, primers NbGAPDH-F and NbGAPDH-R were used to generate 125 bp long amplicon (Bianchi et al., 2015; Tarquini et al., 2019). The same batch of cDNA, synthesized using random primers, was used to amplify GPGV and the reference gene transcripts to minimize inconsistency in qPCR results. RT-qPCR was performed in triplicate (Song et al., 2021), and the cycling conditions were set to allow the melt curve analysis at the end of qPCR. The standard curve was generated according to Song et al. (2021). The relative virus RNA level was calculated using the comparative Cq [2^(-ΔΔCq)] method using amplification on RNA from mock-inoculated plants as a baseline (Bianchi et al., 2015; Tarquini et al., 2019). Infiltrated grapevine plants were considered GPGV positive when their Cq values were below 34, the threshold for a negative test established previously (Bianchi et al., 2015; Tarquini et al., 2019).

2.8. Effect of GPGV clones on grape yield

The yield components of a grapevine plant included the total number of clusters and the weight of the berries in these clusters (de Souza et al., 2019; Ohana-Levi et al., 2024). The cluster number and yield of berries for greenhouse-grown grapevines that were infiltrated with buffer or with one of the wildtype clones (pGPGV-SY, pRI::GPGV-vir, pRI::GPGV-lat) or the mutant clone (pGPGV-SY-C/T) were measured in the second year. A yield assessment was conducted for seven grapevine plants per treatment.

2.9. Statistical analysis

A statistical significance analysis was performed using a generalized linear mixed model (GLMM) using PROC GLIMMIX followed by one-way and two-way analysis of variance (ANOVA). The values for the indicated number of replicates (n) were used to calculate mean and standard error. The sample sizes varied in different experiments. The RT-qPCR of *N. benthamiana* involved six samples each, whereas those of grapevine were five samples each for five different time points. The budburst experiment was conducted with 25 samples in the first year and 15 samples in the second year for each treatment, whereas yield assessment was conducted with seven samples each. Mean difference values obtained within an experiment were determined by Tukey-Kramer HSD tests ($P < 0.05$) using statistical software SAS 9.4 (SAS Institute, USA). A few statistical tests were also conducted using student t-tests (GraphPad Prism). The graphs based on these statistical data were generated using GraphPad Prism 10.2.3.

3. Results

3.1. GPGV isolates of ontario cluster into a single group of a phylogenetic tree

In total, 105 recombinant plasmids derived from RT-PCR were sequenced. These sequences represent GPGV isolates from 21 independent sources that differ in genotype (*V. vinifera*, French-American hybrids, North American grapes), utility (wine grapes, juice grapes, and table grapes) and location. Three isolates, ON93-12 (Syrah), ON560 (Baco) and ON1084 (Sovereign coronation) (Table S1), each contained a single genetic variant, whereas the remaining samples had a mixture of two or more genetic variants. Because many of these plasmids had identical insert sequences, we identified 51 distinct GPGV sequences. We included them in the final phylogenetic tree (Fig. 2A). Also included in the phylogenetic analysis were the corresponding regions of the genome from 16 isolates retrieved from GenBank (first 16 isolates of Table S2). These included two isolates sequenced previously in our lab as part of the large-scale surveys (Xiao et al., 2018). As shown in Fig. 2A, four clades were revealed, which aligns with recent phylogenomic reports (Kaur et al., 2023; Vu et al., 2023). All but three GPGV sequences obtained in this study belonged to clade 2. One sequence each from Seyval blanc (ON1096B), Chambourcin (ON1114C) and Pinot noir (ON384B) belonged to clade 2 (Fig. 2A). Clade predominately included sequences obtained from Italy and Australia, which included isolate fvg-Is-15 (MH087446) originated from an asymptomatic vine in Italy,

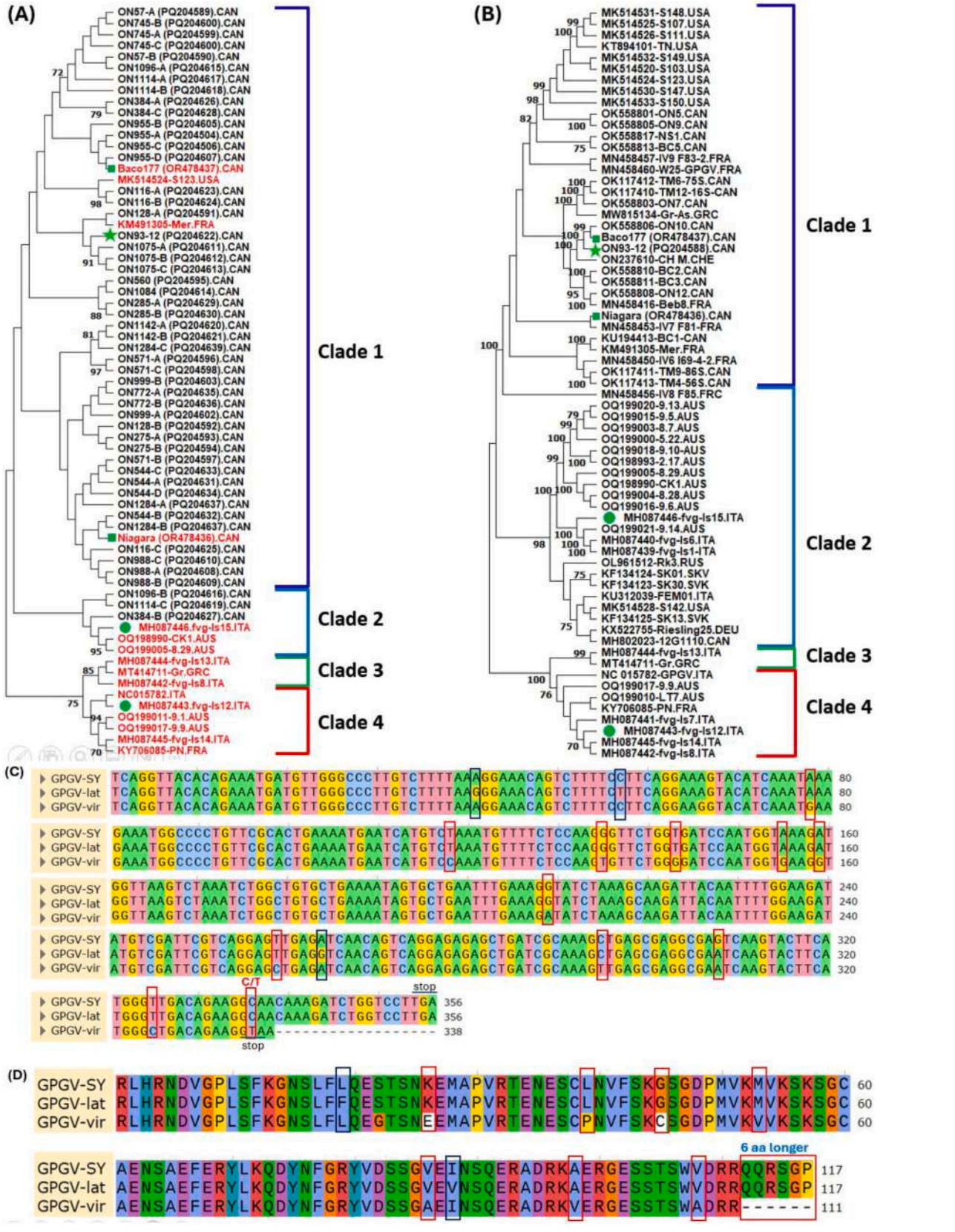

(caption on next page)

Fig. 2. Phylogenetic analysis and sequence alignment of GPGV sequences. **A:** Phylogenetic tree based on the MP/CP gene sequences of 53 GPGV isolates from Ontario (this study) and 16 global GPGV retrieved from GenBank. **B:** Phylogenetic tree based on the genome sequences of three GPGV isolates from Ontario (this study) and 64 global isolates retrieved from GenBank. Phylogenetic analyses were conducted using maximum likelihood. The genome sequence of ACLSV was used as an outgroup. Numbers at the nodes indicate their bootstrap scores. Branches supported by a minimum of 70% of 1000 bootstrap replicates are shown. The isolates depicted with circles were used to construct infectious clones of GPGV by Tarquini et al. (2019), whereby fvg-Is15 was used as the template for pRI::GPGV-lat and fvg-Is12 was used to produce pRI::GPGV-vir. The isolate marked with a green star was used to construct an infectious clone of GPGV in this study, pGPGV-SY. Two additional GPGV isolates sequenced previously in our lab are denoted with green squares. **C:** Multiple alignment of 356 nt long sequences at the 3′ end of the MP of three GPGV clones. This region in pRI::GPGV-vir was swapped with the corresponding sequence from pRI::GPGV-vir to create the pRI::GPGV$_{Chimera}$ in Tarquini et al. (2021a). **D:** Multiple alignments of amino acid sequences encoded by this swapped 356 nts region of ORF2. The differences between pGPGV-SY and pRI::GPGV-lat are marked with blue boxes, whereas those between pRI::GPGV-vir and pRI::GPGV-lat are marked with red boxes. The C/T polymorphic site and stop codons in different variants are indicated. (For interpretation of the references to colour in this figure legend, the reader is referred to the Web version of this article.)

the source for the infectious clone pRI::GPGV-lat (Tarquini et al., 2019). Clade 3 consisted exclusively of European isolates. GPGV isolates in clade 4 comprised isolates from Europe and Australia, all containing a T at the polymorphic site. The Italian isolate fvg-Is-12 (MH087443), originating from a symptomatic grapevine, served as the source for the second infectious clone, pRI::GPGV-vir (Tarquini et al., 2019). Among these four clades, clades 1 and 2 together resembled clade A, clade 3 resembled clade B, and Clade 4 resembled clade D based on the designation scheme provided (Bertazzon et al., 2017). The nucleotide sequence identities of the MP-CP region of Ontario isolates ranged from 97.4% to 99.7%. The overall nucleotide sequence identities of all GPGV isolates ranged from 96.2% to 99.9%.

To corroborate the results above, a phylogenetic analysis of complete or near-complete genome sequence of GPGV, including ON93-12 (PQ204588), Niagara (OR478436) and Baco177 (OR478437), together with an additional 64 GPGV isolates retrieved from GenBank (Table S2), demonstrated the presence of similar 4 clade topology as observed in Fig. 2A, in which Canadian GPGV isolates were clustered in clade 1 consisting of European isolates, mostly of France. The remaining clades consisted primarily of European and Australian isolates (Fig. 2B). The clustering of isolates ON93-12, fvg-Is-15, and fvg-Is-12 follow the same clades mentioned in Fig. 2A. The genomic sequences of the three GPGV isolates from Ontario were 98.6%–99.5% identical, compared to 92.4–99% for all 67 GPGV isolates.

3.2. Construction of a full-length clone of GPGV

Based on results from the phylogenetic analyses, GPGV isolates from Ontario mainly belong to clade 1. Since a cDNA clone representing clade 1 was unavailable, the isolate ON93-12 from Syrah (from now on designated as GPGV-SY) from Ontario, Canada, was chosen as source material for the construction of a full-length cDNA clone because it contained a single GPGV variant (Fig. 1) and genome sequence was made available by HTS using the protocol as mentioned (Xiao et al., 2019). The GPGV-SY clone, when subcloned to the binary vector, was named pGPGV-SY. The mutant clone pGPGV-SY-C/T was generated

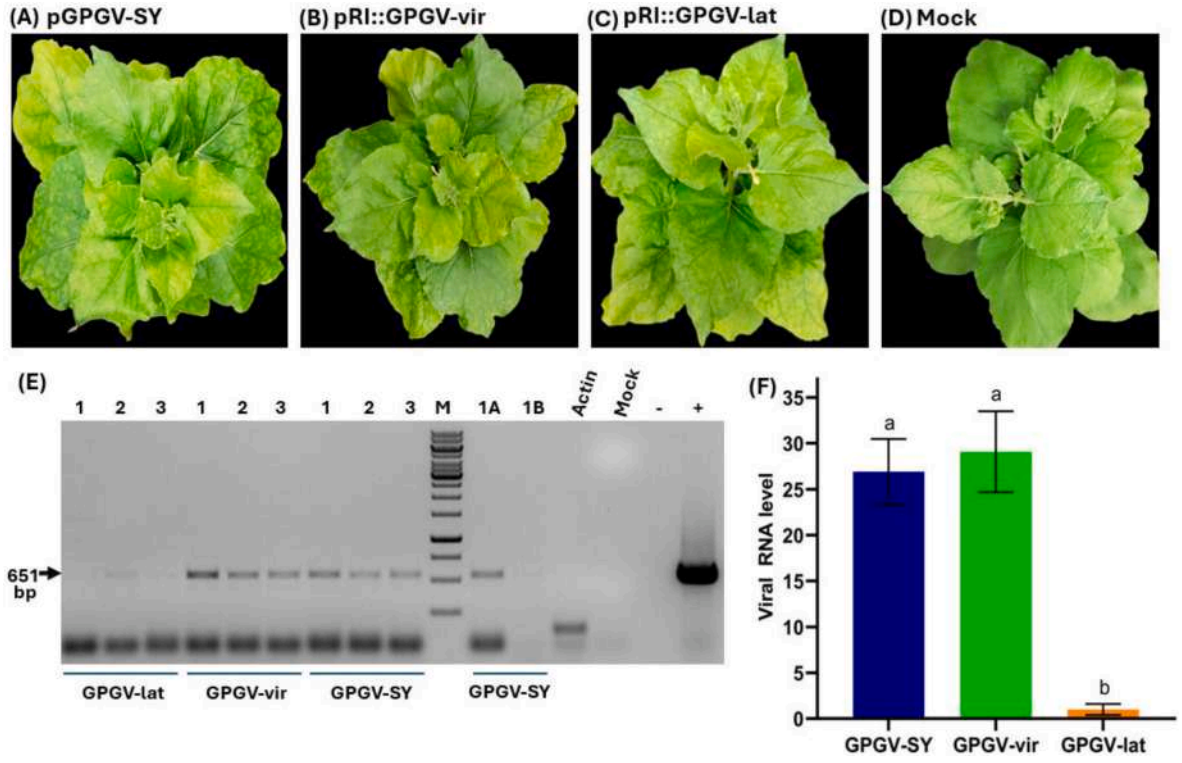

Fig. 3. Assessment of infectivity of wildtype clone of GPGV in *Nicotiana benthamiana* 14 days post infiltration. Mottling and widespread chlorosis symptoms were observed in systemic leaves of *N. benthamiana* by pGPGV-SY **(A),** pRI::GPGV-vir **(B),** pRI::GPGV-lat **(C)**, whereas mock-infiltrated (empty vector) plants were symptomless **(D)**. **E:** Agarose gel electrophoresis of RT-PCR products of GPGV in agro-infiltrated *N. benthamiana* plants. M: 1 kb DNA ladder (GeneRuler), Actin: reference gene for RT-PCR with an amplicon size of 206 bp. GPGV-infiltrated *N. benthamiana* samples were primarily collected at 14 dpi, whereas pGPGV-SY infected samples 1A and 1B were collected at 20 dpi and 28 dpi, respectively. Lane (+): positive control using plasmid DNA for pGPGV-SY as the template. Lane (−): water. **F:** Viral RNA level produced by GPGV clones in leaf tissues of *N. benthamiana*. The bar graphs showed the relative accumulation of viral RNA (mean ± SE) in distal, non-inoculated leaves. Different letters showed a significant difference between treatments.

through Site-directed mutagenesis (SDM) using pGPGV-SY as the template (Fig. 1B). The accuracy of pGPGV-SY and pGPGV-SY-C/T were initially assessed by PCR and restriction digestion, which was then confirmed through DNA sequencing.

3.3. pGPGV-SY causes systemic infection in Nicotiana benthamiana

To rapidly assess if the full-length cDNA clone was biologically active, pGPGV-SY was first infiltrated into the leaves of *N. benthamiana*, an herbaceous experimental host commonly used to test for the infectivity of viral cDNA clones. In a preliminary experiment, we found that infiltration with GPGV clones resulted in low virus RNA content, requiring two rounds of PCR amplification to get a detectable number of RT-PCR products. The infiltration of GPGV clones with RSS p19 (Park et al., 2004; Várallyay et al., 2014) increased the virus concentration and enhanced the symptom severity (Fig. 3A–F). The two GPGV clones, pRI::GPGV-vir and pRI::GPGV-lat that were recently reported (Tarquini et al., 2019) were also used as controls in the infiltration experiment. Ten plants were subjected to agro-infiltration for each viral clone, followed by monitoring symptom development and RT-PCR to detect viral RNA. Three separate experiments were conducted to ensure the reproducibility of results. Mild chlorosis and mottling were first observed in the upper, non-inoculated leaves at 10 days post infiltration (dpi) for pGPGV-SY and pRI::GPGV-vir and at 12 dpi for pRI::GPGV-lat. Symptoms became generally more evident after 14 dpi, remained strong until 21–25 dpi, and disappeared by 30–35 dpi when the inoculated plants had recovered (Fig. 3A–D). *N. benthamiana* plants infiltrated with pGPGV-SY and pRI::GPGV-vir showed more severe symptoms than those infiltrated with pRI::GPGV-lat (Fig. 3).

To detect GPGV RNA in distal leaves due to systemic infection, total RNA was extracted from upper, non-infiltrated leaves at 14 dpi, 20 dpi, and 28 dpi subjected to RT-PCR. As shown in Fig. 3E, DNA bands of size 651 bp, corresponding to the MP-CP region, were obtained in all GPGV-infiltrated samples. It is worth noting that the intensity of the PCR products differed between GPGV clones. A faint band was detected in samples infiltrated with pRI::GPGV-lat. In contrast, much stronger bands were detected for pRI::GPGV-vir and pGPGV-SY (Fig. 3E). Among the 10 agroinfiltrated plants for each clone, 6 plants were randomly selected, and their GPGV RNA levels were assessed using RT-qPCR. As shown in Fig. 3F, viral RNA levels in the systemic leaves infiltrated with pRI::GPGV-lat differed significantly from those infiltrated with either pRI::GPGV-vir or pGPGV-SY ($F = 135.4$, $p < 0.001$). For example, the mean viral RNA level in *N. benthamiana* leaves infiltrated with pRI::GPGV-lat was 1 ± 0.25 as compared to 29 ± 1.75 for pRI::GPGV-vir and 27 ± 1.46 for pGPGV-SY. Viral RNA levels due to pRI::GPGV-vir and pGPGV-SY were not significantly different (Fig. 3F). As expected, the mock control, which was *N. benthamiana* plants infiltrated with empty pCB301 vectors, remained symptomless and tested negative with the RT-PCR assay. This thorough data analysis provides a solid basis for conducting GPGV infectivity assay in grapevine.

3.4. Effects of grapevine cultivars on the infectivity of GPGV clones

Utilizing the optimized protocol that was recently developed in our lab (Shabanian et al., 2023), we compared the infectivity and pathological properties of pGPGV-SY with the two viral cDNA clones constructed by Tarquini et al. (2019). Because co-infiltration with a potent RSS was critical in launching grapevine infection using full-length viral cDNA clones (Shabanian et al., 2023 and this study), we included a plasmid vector expressing p19 (Park et al., 2004; Várallyay et al., 2014) in all grapevine infiltration experiments. To test if any difference exists between grapevine cultivars in the infectivity of GPGV cDNA clones, we infiltrated each GPGV clone together with p19 into Cabernet franc (CF) and Syrah (SY), followed by symptom observation and molecular tests. As shown in Fig. 4, the infiltrated CF plants contained significantly higher levels of viral RNA compared to SY plants for both pGPGV-SY [$F = 63.34$, $P = 0.0005$ (Fig. 4A)] and pRI::GPGV-vir [$F = 59.04$, $P = 0.0001$ (Fig. 4B)] at both time points assayed (5 and 17 mpi). For example, CF plants infiltrated with pGPGV-SY had viral RNA levels that were 6.2-fold higher at 5 months post infiltration (mpi) and 5.8-fold higher at 17 mpi compared to Syrah plants (Fig. 4A). A similar trend was observed for the two cultivars that were infiltrated with pRI::GPGV-vir (Fig. 4B). Further, a higher percentage of CF plants showed symptoms which were also more severe compared to SY grapevines infiltrated with either pGPGV-SY or pRI::GPGV-vir (Fig. 4C). For these reasons, CF was selected and used in all subsequent experiments.

3.5. Comparative analyses of three GPGV clones in grapevine

Two separate infiltration experiments were conducted with each of the three GPGV cDNA clones. In total, 37 CF plantlets were infiltrated with each viral clone. The percentage of surviving plants ranged from 73 to 78%. After infiltration, the CF grapevines were monitored over three years to obtain a comprehensive idea of disease progression and the temporal kinetics of GPGV replication. Disease symptoms were catalogued using the same criteria established in previous research for consistency (Tarquini et al., 2018; Messmer et al., 2023). Mild GLMD symptoms included light chlorosis and mottling, as observed in grapevines infected with pRI::GPGV-lat (Fig. 5D) and a few grapevine plants pGPGV-SY and pRI::GPGV-vir. In contrast, severe GLMD symptoms included extensive leaf mottling (Fig. 5B–C, E-H), deformed leaves (Fig. 5B and CE-H), shorter internodes (Fig. 5B–C, F-G), and zigzag and stunted growth (Fig. 5F–G) were mainly observed in pGPGV-SY and pRI::GPGV-vir infected grapevines. These symptoms were comparable with those reported by others under greenhouse (Tarquini et al., 2019b, 2021a) or field conditions (Bertazzon et al., 2017; Messmer et al., 2023;

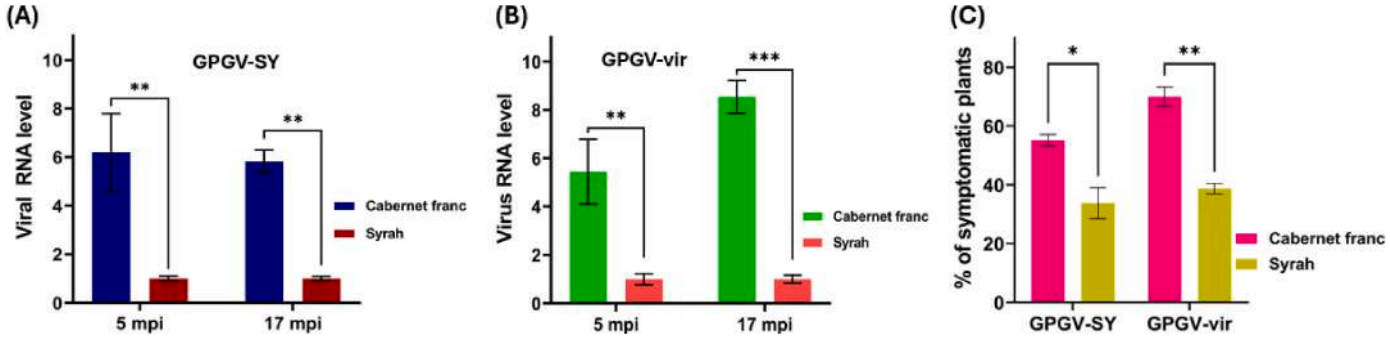

Fig. 4. Optimization of the infectivity of GPGV full-length clones in grapevine. The relative levels of GPGV RNA in grapevines infiltrated with pGPGV-SY **(A)** and pRI::GPGV-vir **(B)** of Cabernet franc and Syrah were measured at 5 and 17 months post infiltration. **C:** Percentage of grapevine plants showing GLMD symptoms after infiltration with pGPGV-SY or pRI::GPGV-vir. The error bar in each group represents the standard error of the mean, and the asterisks denote statistically significant differences at different levels: * significance at $P \leq 0.05$; ** significance at $P \leq 0.01$; and *** significance at $P \leq 0.001$.

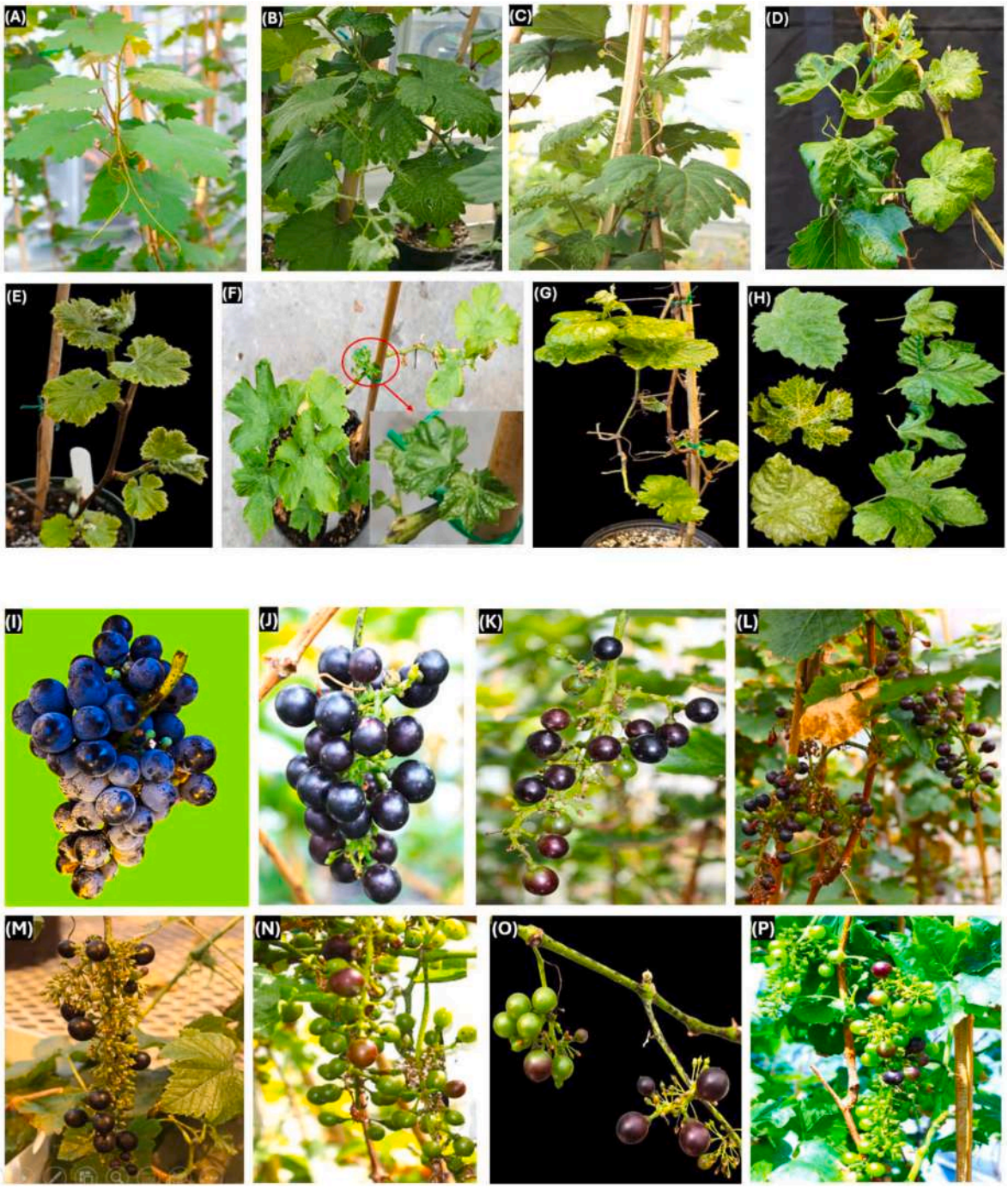

Fig. 5. Representative symptoms observed in *Vitis vinifera* cv. Cabernet franc after agroinfiltration with three grapevine Pinot gris virus cDNA clones. Characteristic symptoms on grapevine leaves due to GPGV infection are shown in B-H, whereas those on berries and berry clusters are shown in J-P. **A & I:** Grapevines agro-infiltrated with an empty vector as a mock. **B & D:** Mottling and deformation of leaves, shorter internodes and zigzag growth of grapevine infiltrated with pGPGV-SY, pRI::GPGV-vir, and pRI::GPGV-lat, respectively. **E-H:** Additional pGPGV-SY infiltrated grapevines with GLMD symptoms with chlorotic and mottled leaves immediately after budburst in infiltrated-grapevine (**E**), leaf mottling, shorter internode, stunting, and poor plant growth (**F**), leaf deformation, zigzag growth and stunting (**G**), leaf mottling and deformation (**H**). **J &L:** Ripe berries with relatively loose clusters collected from grapevines infiltrated with pRI::GPGV-lat, pGPGV-SY, and pRI-GPGV-vir, respectively. **K:** Uneven ripening and thin cluster due to infection of pGPGV-SY. **(M)** Additional effects on grape yield included loose clusters with millerandage of berries (**M**), abnormal shapes, delayed and immature ripening of berries **(N)**, similar clusters with small berries along with unfertilized flowers (**O**), and uneven fruit set (**P**). The A-D pictures were taken at 4.5 mpi, **E** at 16 mpi, **F &H** at 6 mpi, **I & N** at 20 mpi, and **O-P** at 19 mpi.

Saldarelli et al., 2015). All three GPGV clones elicited symptoms but differed in the speed of symptom development, the percentage of symptomatic plants, the percentage of plants with severe symptoms, and the time to recover. For example, 2 of 28 plants infiltrated with pRI::GPGV-vir first showed GLMD symptoms at 2.5 mpi, and 3 of 29 plants infiltrated with pGPGV-SY first developed symptoms after a two-week delay. In contrast, GLMD symptoms were first observed at 3.5 mpi in only one of 28 grapevines infiltrated with pRI::GPGV-lat. The total number of symptomatic plants and plants exhibiting severe symptoms varied between GPGV clones and with time-lapse post-infiltration and the growth stages of grapevines to some extent. For example, at 5 mpi, the percentage of symptomatic plants for pRI::GPGV-vir, pGPGV-SY, and

pRI::GPGV-lat was 71%, 52%, and 26%, respectively, whereas the corresponding values for severe symptoms were 54%, 38%, and 11% (Table 1).

These three GPGV cDNA clones also differed in the time they took for the infected grapevine to recover from symptoms. For example, most symptomatic plants infiltrated with pRI::GPGV-lat recovered by 4 mpi, whereby new shoots developed longer internodes and healthy-looking leaves. Nine plants infiltrated with pGPGV-SY and three infiltrated with pRI::GPGV-vir showed symptom recovery by 4.5 mpi, whereas 4 plants infiltrated with pGPGV-SY and 2 plants infiltrated with pRI::GPGV-vir retained symptomatic on newly developed shoots until up to 5.5 mpi and 6 mpi, respectively. However, a few severely infected plants retained mild symptoms beyond this point, especially on lower branches that were not exposed to direct light because of shade. As expected, mock control grapevines remained asymptomatic for the entire observation period. Taken together, grapevines infiltrated with pGPGV-lat recovered sooner, followed by those infiltrated with pGPGV-SY, whereas those infiltrated with pRI::GPGV-vir took the longest time to recover from symptoms.

RT-PCR was conducted on all surviving plants at five time points (3, 5, 7, 9, and 17 mpi) to assess differences in the infectivity rate between these three clones. However, noticeable differences were observed at 5 mpi, 9 mpi, and 17 mpi; hence, these time points were used for RT-PCR-based assessments. It is clear that at each time point, the number of plants tested positive for pGPGV-SY or pRI::GPGV-vir was significantly higher than the number of plants infiltrated with pRI::GPGV-lat. For example, the percentage of GPGV-positive grapevine infiltrated with pGPGV-SY ranged from 61.8% at 5 mpi, 49.3% at 9 mpi, and 63.9% at 17 mpi and the GPGV-positive plants for pRI::GPGV-vir at the same time points were 61.7%, 36.7%, and 45%, respectively (Fig. 6A). In contrast, the percentages of positive plants infiltrated with GPGV-lat were much lower, at 16.4%, 8%, and 12.1% for the same three-time points, respectively (Fig. 6A). Interestingly, regardless of the GPGV clones used in infiltration, the number of grapevines tested positive for GPGV was the highest at 17 mpi, likely a reflection of enhanced viral replication in new tissues that emerged after dormancy culminating in GPGV RNA levels that RT-PCR could readily detect.

RT-qPCR analyses examined the relative viral RNA levels in grapevines infiltrated with the three GPGV clones at the same five-time points. As shown in Fig. 6B, a similar temporal trend emerged for all GPGV clones: RNA levels peaked at 5 mpi, then gradually declined until 9 mpi, then rose again to 17 mpi. The only exception was pRI::GPGV-vir, which had the highest level of viral RNA at 3 mpi instead. Two-way ANOVA analysis suggested that the differences between the five-time points were significant for each clone. When RNA levels among the three GPGV clones were compared using one-way ANOVA, it was shown that both pGPGV-SY and pRI::GPGV-vir produced significantly higher levels of viral RNA than pRI::GPGV-lat at each time point (Fig. 6B). For example, the viral RNA level in grapevines infiltrated with pGPGV-SY was 14.7-fold higher at 3 mpi and 16.8-fold higher at 5 mpi when compared to the same points in plants infiltrated with pRI::GPGV-lat (Fig. 6B). The corresponding fold change differences of pRI::GPGV-vir relative to pRI::GPGV-lat were 16.6 fold at 3 mpi and 15.8 fold at 5 mpi (Fig. 6B). The fold change values for pGPGV-SY at 9 mpi and 17 mpi were 9.4 fold and 15.6 fold, slightly higher than the corresponding values for pRI::GPGV-vir, which were 7.1 fold and 13.9 fold, thus showing differential virus titre before and after the symptom recovery between these two clones. Furthermore, one-way ANOVA was conducted to examine the differences in the cumulative RNA values by three viral clones, which showed significantly lower virus RNA level by pRI::GPGV-lat compared to pGPGV-SY and pRI::GPGV-vir ($P < 0.0001$). Again, RNA accumulation by pGPGV-SY and pRI::GPGV-vir did not differ statistically (Fig. 6C). However, the average RNA level of pGPGV-SY (13.66 ± 1.1) was slightly higher than pRI::GPGV-vir (12.66 ± 1.4) (Fig. 6C). Grapevines infiltrated with pGPGV-lat recovered sooner (4–5 mpi), whereas those infiltrated with pRI::GPGV-vir took the longest time (4.5–6 mpi) to recover from symptoms. Even a few severely infected plants remained symptomatic throughout. Thus, the severity of symptoms of grapevines infected with the three GPGV clones correlated well with the RT-qPCR results.

In addition to the foliar symptoms described above, infection with GPGV clones also had different degrees of adverse effects on fruit set, the number and size of grape clusters, fruit ripening and yield. Representative images depicting the impact of infection with the three GPGV clones on cluster number and yield as a percentage of the values determined for mock-infiltrated grapevines are shown in Figs. 5 and 6. A significant reduction in cluster numbers was observed in grapevines infected with three GPGV clones ($F = 8.20$, $P = 0.0057$). For example, pGPGV-SY (61.4 ± 5.4) and pRI::GPGV-vir (65.91 ± 6.4) caused a significant reduction in the number of clusters per vine compared to pRI::GPGV-lat (84.09 ± 4.5) (Fig. 6E). However, no significant difference in cluster numbers was observed between pGPGV-SY and pRI::GPGV-vir. Similar results were observed for the effect of three viral clones on yield ($F = 12.77$, $P = 0.0001$) (Fig. 6F). Infection with pRI::GPGV-lat had the slightest impact as it caused 21.1% reduction. In contrast, corresponding values for pRI::GPGV-vir and pGPGV-SY were 39.9% and 45.4%, respectively. In contrast, infection with GPGV-SY and GPGV-vir had significantly increased effects. Again, the effects on yield due to pGPGV-SY and pRI::GPGV-vir did not differ significantly (Fig. 6F).

Table 1
Survival and symptom development of GPGV in *V. vinifera* cv. Cabernet franc as observed in two independent experiments.

Treatments	*Vitis vinifera* cv. Cabernet franc			
	Infiltrated	Survived (5 mpi)	Symptomatic (5 mpi)	Severe symptoms (5 mpi)
pGPGV-SY	37 (20 + 17)	29 (15 + 14)	15	11
pGPGV-SY-C/T	37 (20 + 17)	27 (15 + 12)	22	17
pRI::GPGV-vir	37 (20 + 17)	28 (16 + 12)	19	15
pRI::GPGV-lat	32 (15 + 17)	27 (13 + 14)	7	3
MOCK	37 (20 + 17)	34 (18 + 16)	0	0

3.6. The C to T mutation of GPGV-SY results in enhanced virulence and disease severity

To put to rest the long-standing contention that the C/T polymorphism in GPGV ORF2 encoding MP may be responsible for different outcomes of infection by GPGV variants belonging to different phylogroups (i.e. asymptomatic vs. symptomatic), a mutant clone pGPGV-SY-C/T was generated via SDM to replace the cytidine at genomic position 6685 with thymidine. This mutant virus would encode an MP that is six amino acids shorter than the wildtype virus (Fig. 1B). The effects of this point mutation on viral RNA accumulation and disease symptoms were investigated in the natural host through agroinfiltration. As a result, Cabernet franc plants infiltrated with the wildtype clone developed symptoms in 52% of the surviving plants, and 38% exhibited severe symptoms (Table 1). In contrast, among the 27 grapevines that survived after infiltration with pGPGV-SY-C/T, 81.5% developed GLMD symptoms, and 63% developed severe symptoms (Table 1). Symptoms characteristic of GPGV infection were first observed at 2.5 mpi in five plants infiltrated with the mutant clone. They included severe chlorosis, extensive mottling and deformation of leaf blades, shortened internodes, and zigzag growth in some plants. The impact of the C/T mutation on viral infectivity was studied first by RT-PCR, which showed a significantly higher percentage of GPGV-positive plants ($F = 25.83$, $P = 0.0023$) after infiltration with pGPGV-SY-C/T compared to the wildtype

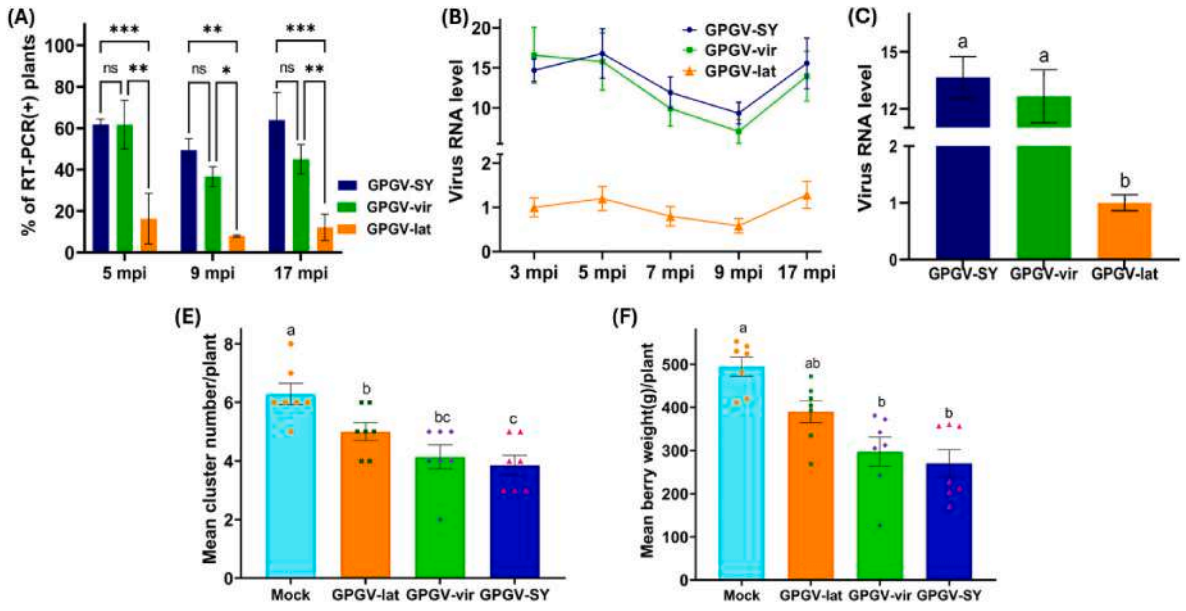

Fig. 6. Comparative assessment of GPGV clones in *V. vinifera* cv. Cabernet franc. **A:** Percentage of RT-PCR-positive plants infected with pGPGV-SY, pRI::GPGV-vir, or pRI::GPGV-lat at 5, 9, and 17 mpi. **B:** Quantitative assessments of the ΔCq for GPGV RNA in grapevines infected with three GPGV clones and mock at the first three points, especially to check whether all the grapevines infiltrated with pRI::GPGV-lat were infected as the majority of the plants were symptomless and only a few plants tested positive by RT-PCR. **C:** Cumulative GPGV RNA level in grapevines infiltrated with three GPGV clones. **D:** Effects of infection with three GPGV clones on the number of clusters in the second year of plant growth. **E:** Effects of infection with three GPGV clones in the second year of plant growth. The length of the bar is the mean value. Brackets indicate mean ± SE. Means denoted by a different letter indicate significant differences between treatments ($p < 0.05$, Tukey–Kramer method). $n = 7$ per treatment. ns: not significant $P > 0.05$). * Significant ($P \leq 0.05$); ** significant ($P \leq 0.01$).

clone pGPGV-SY at both 9 ($P = 0.0483$) and 17 mpi ($P = 0.0461$) (Fig. 7A). This indicated that pGPGV-SY-C/T was more virulent than pGPGV-SY. Further assessment by RT-qPCR showed a significant difference between the mutant and the wildtype clones ($F = 81.83$, $P < 0.0001$). Significantly higher viral RNA levels from pGPGV-SY-C/T over pGPGV-SY were observed at each time point used for assessment (Fig. 7B).

As shown in Fig. 7C, the number of grapevine clusters infiltrated with pGPGV-SY-C/T was slightly lower than in grapevines infiltrated with the wildtype clone. However, this difference was not statistically significant. In stark contrast, infection with pGPGV-SY-C/T, causing a yield reduction of up to 60.4%, had a significantly higher effect on grape yield ($P = 0.0368$) compared to pGPGV-SY with a yield reduction of 45.4% (Fig. 7D). Collectively, these data suggest that a single C to T mutation at this polymorphic site enhanced the virus's infectivity, resulting in significant increases not only in RNA accumulation but also in the percentage of plants developing symptoms, disease severity, and yield loss.

4. Discussion

GPGV exhibits a complex etiology due to its complicated association with GLMD disease, as GLMD symptoms are only expressed only in a few grapevine cultivars in field conditions and are caused mainly by the infection of GPGV variants from the clade 4 (formerly clade C) (Bertazzon et al., 2017; Saldarelli et al., 2015; Vu et al., 2023). In contrast, GPGV variants from other clades are associated with no or mild symptoms (Bertazzon et al., 2017; Saldarelli et al., 2015; Messmer et al., 2023). The conclusive evidence regarding GLMD etiology, the pathogenesis of GPGV, its interaction with grapevine hosts, and underlying molecular mechanisms governing the different aspects of the GPGV viral replication cycle had remained virtually unknown, primarily due to the unavailability of infectious clones of GPGV and the need for efficient experimental systems to initiate infections with viral clones in virus-free grapevines until recently. When this project was initiated, no full-length clones were available for GPGV isolates. As this research was ongoing, Tarquini et al. (2019) reported the construction of two full-length cDNA clones of GPGV, one representing the asymptomatic lineage (now clade 1) and the other representing the symptomatic lineage (now clade 4). Unfortunately, they designated these cDNA clones pRI::GPGV-lat and pRI::GPGV-vir, respectively, as such designations are misleading. Phylogenetic analysis revealed that GPGV diversity in Ontario, Canada, is relatively small, and all except three GPGV sequences we obtained clustered in clade 1 together with North American and French isolates. However, GPGV isolates from diverse population structures, including groups of grapevines, including wine grapes, hybrid grapes, and wild grapes, were used for assessment. The 651 bp long sequence of MP-CP region of the remaining three GPGV clones from Ontario, Canada, were clustered in clade 2, containing predominantly Italian isolates, including the source for pRI::GPGV-lat. These results suggest that GPGV isolates in Ontario, Canada, likely originated from Europe, particularly France. This conjecture is reasonable as most grapevine planting materials grown commercially in Canada were imported from France (Vu et al., 2023).

The isolate ON93-12 from Syrah was chosen as the source for constructing an infectious clone, pGPGV-SY, to represent clade 1. We subsequently demonstrated that pGPGV-SY was infectious and caused systemic infections in the experimental host *N. benthamiana*. Though chlorosis and mottling were frequently observed on the upper, non-inoculated leaves, these symptoms were often subtle and could not be a reliable indicator of infection. Therefore, infection status was confirmed with RT-qPCR, and the results showed that GPGV was present but replicates rather slowly, a feature shared by the two Italian clones (Tarquini et al., 2019).

We subsequently tested pGPGV-SY for its infectivity, replication kinetics and pathological properties in grapevine, the natural host of GPGV. The genome sequence of pGPGV-SY is more closely related to pRI::GPGV-lat than to pRI::GPGV-vir, so it was expected that pGPGV-SY would behave more like pRI::GPGV-lat when inoculated into grapevine. We demonstrated yield reduction ranging from 21.1% to 59.5% in controlled conditions. In field conditions, the yield reduction ranged from 13% to 96%, and the reduction occurred only in symptomatic vines (Messmer et al., 2023). Surprisingly, pGPGV-SY was much more

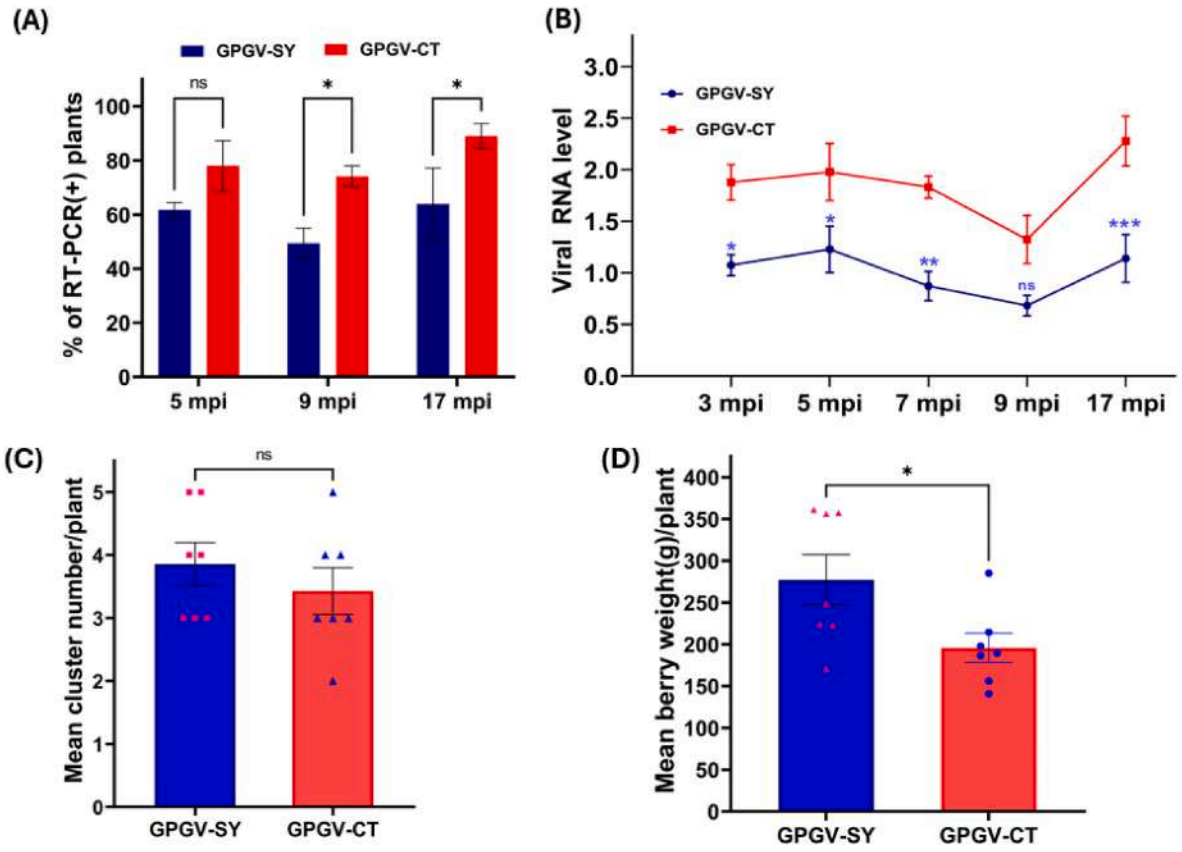

Fig. 7. Comparative assessment of pSY-GPGV-C/T (denoted in figure by GPGV-CT) in *V. vinifera* cv. Cabernet franc. Symptoms elicited by pGPGV-SY-C/T infection include **A:** Percentage of RT-PCR positive plants infiltrated with pGPGV-SY or pGPGV-SY-C/T at 5, 9, and 17 mpi; **B:** A quantitative assessment of the virus RNA level in grapevines infiltrated with pGPGV-SY or pGPGV-SY-C/T clones at different time points; **C:** The effect of pGPGV-SY and pGPGV-SY-C/T clones on the number of clusters per vine measured in the second year of plant growth; **D:** The impact of pGPGV-SY and pGPGV-SY-C/T clones on grape yield measured in the second year of plant growth. The length of the bar is the mean value. Means denoted by a different letter indicate significant differences between treatments ($p < 0.05$, Tukey–Kramer method). n = 7 per treatment. Brackets indicate mean ± SEM * Significant ($P \leq 0.05$); ** significant ($P \leq 0.01$); *** significant ($P \leq 0.001$).

aggressive than pRI::GPGV-lat, although they are genetically more closely related and encode the longer MP. This conclusion was based on multiple criteria, including infection rate, percentage of grapes developing symptoms, RNA levels, and the secondary effects of infection, such as size and number of clusters, fruit yield, delays in budburst and a smaller number of open buds (Table S4). In fact, pGPGV-SY behaved more like pRI::GPGV-vir, though the latter encoded a shorter MP and originated from a symptomatic source. These results question the validity of the proposed correlation between phylogenetic affinity and infection outcomes, as initially suggested (Saldarelli et al., 2015), which was supported by the infectivity assays of two Italian clones (Tarquini et al., 2019, 2021a).

Our phylogenetic analyses agree with splitting the former clade A of Bertazzon et al. (2017) into two clades, clades 1 and 2, to ensure consistency (Vu et al., 2023). Within these two clades, the isolate ON93-12 (GPGV-SY) belongs to clade 1, whereas isolate fvg-Is15 (pRI::GPGV-lat) falls into clade 2 (Fig. 1A–B). Closer examination revealed that these two isolates share 98.75% identity in the nucleotide sequence, with 87 mismatches distributed across the genome. Some of these differences are responsible for the differences in viral RNA levels and symptom development between the two viral cDNA clones.

A major distinction between variants of different lineages of GPGV variants is the polymorphic site near the end of ORF2, resulting in two versions of MP that differ in size. Specifically, all variants from clades 1 and 2 have a cytosine at genomic position 6685 and would encode an MP of 375 amino acids. In contrast, variants of clade 4 contain uracil instead and would encode an MP that is six amino acids shorter due to the emergence of an early stop codon. It was hypothesized that the shorter MP may be the genetic determinant for symptomatic infections, whereas the longer MP is associated with asymptomatic or mild infections (Bertazzon et al., 2017; Saldarelli et al., 2015). However, experimental evidence from this work and others refutes this hypothesis. Recently, Tarquini et al. (2021a) made a chimeric clone (pRI::$GPGV_{Chimera}$) by swapping a 356 bp region corresponding to the 3′ region of ORF2 in GPGV-vir with a synthetic DNA fragment based on the sequence of GPGV-lat. This chimeric clone would encode the MP larger by six amino acids than pRI::GPGV-vir. When inoculated into Kober 5BB, a commonly used grapevine rootstock, this chimeric clone behaved more like GPGV-lat: it accumulated viral RNA at a level that was 25-fold lower compared to the parent clone GPGV-vir (Tarquini et al., 2021a). It is important to note that when the swapped regions were compared, their corresponding peptides differed by 16 aa residues. Therefore, the difference between the mutant and the parent GPGV clones cannot be attributed solely to this site's T to C mutation.

We wanted to test the precise effect of this single-point mutation on viral replication and disease phenotype. To this end, a C to T mutation was introduced into pGPGV-SY, and its impact on symptom severity and viral RNA accumulation was tested. This mutant clone caused infection in a higher percentage of grapevines and more severe disease, and the infected plants accumulated 1.7–2.1 times higher levels of viral RNA than the parent clone (Table 1). It would be informative to make a mutant clone of pRI::GPGV-vir, which contained a single mutation from T to C. Follow-up testing of its effects on GPGV replication and symptom development would reveal the impact of a single T to C mutation as observed in a clade 4.

Integrating findings from this and other research (Bertazzon et al.,

2017; Tarquini et al., 2019b, 2021a), we propose a working model to explain the etiological relationship between different GPGV variants and the disease GLMD. As for many plant viruses, the outcome of GPGV infection is influenced by several factors, such as grapevine cultivars, viral strains, other viruses co-inhabiting the same grapevine, and environmental conditions. It is not the genetic lineage of GPGV variants *per se* that determines the outcome of an infection. Instead, the viral titre of GPGV triggers the onset of symptoms. In other words, regardless of the variants involved, infection with GPGV will ultimately develop GLMD symptoms once the viral titre reaches a certain threshold. However, the speed of viral replication varies between different lineages of GPGV variants that would influence the timing and severity of symptoms. For example, variants of clade 4 may replicate faster and reach this threshold sooner. Consequently, grapevine infected with these variants would manifest disease symptoms sooner, in more plants and more profoundly. On the other hand, GPGV isolates of clades 1 and 2 would replicate at a slower pace and take longer to reach this threshold; consequently, they may manifest milder or even no symptoms depending on the titre they attain at a given time. Other factors, such as the load of the inoculum, grapevine cultivars, and environmental conditions, may also influence viral replication and disease progression.

5. Conclusions

In conclusion, we have created a full-length clone representing GPGV clade 1 variants from Ontario. A primary objective of this research is to provide a direct and comprehensive comparison of these clones representing three GPGV lineages in terms of infectivity, replication and pathogenicity when inoculated into grapevine. pGPGV-SY is surprisingly more aggressive than pRI::GPGV-lat. In fact, it behaved more similarly to pRI::GPGV-vir, and as it replicates to much higher levels, it causes more severe symptoms in the grapevine. Moreover, we have demonstrated that a single C to T mutation in the MP gene further enhanced the virulence of the virus. The availability of this and other infectious clones and the grapevine infection system reported here would enable diverse fundamental studies on GPGV, such as pathogenesis, replication and virus-host interactions. In turn, studies on GPGV would help advance our knowledge of the genus Trichovirus, a group of economically important pathogens of woody fruit crops that is much under-studied.

CRediT authorship contribution statement

Dipendra Karki: Writing – review & editing, Writing – original draft, Validation, Project administration, Methodology, Investigation, Formal analysis, Data curation, Conceptualization. **Rita Musetti:** Writing – review & editing, Resources. **Baozhong Meng:** Writing – review & editing, Validation, Supervision, Resources, Project administration, Funding acquisition, Formal analysis, Conceptualization.

Data availability

The partial and complete genome sequences of GPGV isolates of Ontario, Canada, were submitted to the NCBI database with accession numbers PQ204588-PQ204610.

Funding

This research was funded by the Natural Sciences Engineering Research Council of Canada, Discovery Grant Program Projects RGPIN-2014-05306 and RGPIN-2020-04718, awarded to BM.

Declaration of competing interest

The authors declare that they have no known competing financial interests or personal relationships that could have appeared to influence the work reported in this paper.

Acknowledgements

We thank M. Mucci, phytotron coordinator at the Phytotron Facility at the University of Guelph, for her advice and assistance in maintaining the grapevines. We thank Dr. G. Tarquini for sharing technical information on the Italian GPGV clones. We thank Dr. A. Nassuth for her critical review of the manuscript and invaluable comments and suggestions.

Appendix A. Supplementary data

Supplementary data to this article can be found online at https://doi.org/10.1016/j.virol.2024.110360.

References

Angelini, E., Bazzo, I., Bertazzon, N., Filippin, L., Forte, V., 2015. A new disease in Italian vineyards. Wines Vines 55–59.

Bertazzon, N., Forte, V., Angelini, E., 2020. Fast transmission of grapevine "Pinot gris" virus (GPGV) in vineyard. Vitis - J. Grapevine Res. 59, 29–34. https://doi.org/10.5073/vitis.2020.59.29-34.

Bertazzon, N., Forte, V., Filippin, L., Causin, R., Maixner, M., Angelini, E., Fajardo, T.V. M., Silva, F.N., Eiras, M., Nickel, O., 2017. Association between genetic variability and titre of Grapevine Pinot gris virus with disease symptoms. Plant Pathol. 66, 949–959. https://doi.org/10.1111/ppa.12639.

Bianchi, G.L., De Amicis, F., De Sabbata, L., Di Bernardo, N., Governatori, G., Nonino, F., Prete, G., Marrazzo, T., Versolatto, S., Frausin, C., 2015. Occurrence of grapevine pinot gris virus in friuli venezia giulia (Italy): field monitoring and virus quantification by real-time RT-PCR. EPPO Bull. 45, 22–32. https://doi.org/10.1111/epp.12196.

Cieniewicz, E.J., Qiu, W., Saldarelli, P., Fuchs, M., 2020. Believing is seeing: lessons from emerging viruses in grapevine. J. Plant Pathol. https://doi.org/10.1007/s42161-019-00484-3.

Demian, E., Jaksa-Czotter, N., Varallyay, E., 2022. Grapevine pinot gris virus is present in different non-vitis hosts. Plants 11. https://doi.org/10.3390/plants11141830.

de Souza, C.R., da Mota, R.V., Silva, C.P.C., Raimundo, R.H.P., Fernandes, F. de P., Peregrino, I., 2019. Row orientation effects on Syrah grapevine performance during winter growing season. Rev. Ceres 66, 184–190. https://doi.org/10.1590/0034-737X201966030004.

Fajardo, T.V.M., Silva, F.N., Eiras, M., Nickel, O., 2017. High-throughput sequencing applied for the identification of viruses infecting grapevines in Brazil and genetic variability analysis. Trop Plant Pathol 42, 250–260. https://doi.org/10.1007/s40858-017-0142-8.

Giampetruzzi, A., Roumi, V., Roberto, R., Malossini, U., Yoshikawa, N., La Notte, P., Terlizzi, F., Credi, R., Saldarelli, P., 2012. A new grapevine virus discovered by deep sequencing of virus- and viroid-derived small RNAs in Cv Pinot gris. Virus Res. 163, 262–268. https://doi.org/10.1016/j.virusres.2011.10.010.

Glasa, M., Predajňa, L., Šoltys, K., Sabanadzovic, S., Olmos, A., 2015. Detection and molecular characterisation of grapevine Syrah virus-1 isolates from central Europe. Virus Gene. 51, 112–121. https://doi.org/10.1007/s11262-015-1201-1.

Goetz, J.A., Kuehfuss, N.M., Botschner, A.J., Zhu, S., Thompson, L.K., Cox, G., 2022. Exploring functional interplay amongst Escherichia coli efflux pumps. Microbiology (United Kingdom) 168, 1–12. https://doi.org/10.1099/mic.0.001261.

Gualandri, V., Asquini, E., Bianchedi, P., Covelli, L., Brilli, M., Malossini, U., Bragagna, P., Saldarelli, P., Si-Ammour, A., 2017. Identification of herbaceous hosts of the Grapevine Pinot gris virus (GPGV). Eur. J. Plant Pathol. 147, 21–25. https://doi.org/10.1007/s10658-016-0989-4.

Hily, J.M., Komar, V., Poulicard, N., Vigne, E., Jacquet, O., Protet, N., Spilmont, A.S., Lemaire, O., 2021. Biological evidence and molecular modeling of a grapevine pinot gris virus outbreak in a vineyard. Phytobiomes J. 5, 464–472. https://doi.org/10.1094/PBIOMES-11-20-0079-R.

Hily, J.M., Poulicard, N., Candresse, T., Vigne, E., Beuve, M., Renault, L., Velt, A., Spilmont, A.S., Lemaire, O., 2020. Datamining, genetic diversity analyses, and phylogeographic reconstructions redefine the worldwide evolutionary history of grapevine pinot gris virus and grapevine berry inner necrosis virus. Phytobiomes J. 4, 165–177. https://doi.org/10.1094/PBIOMES-10-19-0061-R.

Kaur, K., Rinaldo, A., Lovelock, D., Rodoni, B., Constable, F., 2023. The genetic variability of grapevine Pinot gris virus (GPGV) in Australia. Virol. J. 20. https://doi.org/10.1186/s12985-023-02171-3.

Kurth, E.G., Peremyslov, V.V., Prokhnevsky, A.I., Kasschau, K.D., Miller, M., Carrington, J.C., Dolja, V.V., 2012. Virus-derived gene expression and RNA interference vector for grapevine. J. Virol. 86, 6002–6009. https://doi.org/10.1128/jvi.00436-12.

Liu, K., Yang, Q., Yang, T., Wu, Y., Wang, G., Yang, F., Wang, R., Lin, X., Li, G., 2019. Development of Agrobacterium-mediated transient expression system in Caragana intermedia and characterization of CiDREB1C in stress response. BMC Plant Biol. 19. https://doi.org/10.1186/s12870-019-1800-4.

Lucas, W.J., 2006. Plant viral movement proteins: agents for cell-to-cell trafficking of viral genomes. Virology 344, 169–184. https://doi.org/10.1016/j.virol.2005.09.026.

Malagnini, V., de Lillo, E., Saldarelli, P., Beber, R., Duso, C., Raiola, A., Zanotelli, L., Valenzano, D., Giampetruzzi, A., Morelli, M., Ratti, C., Causin, R., Gualandri, V., 2016. Transmission of grapevine Pinot gris virus by Colomerus vitis (Acari: Eriophyidae) to grapevine. Arch. Virol. 161, 2595–2599. https://doi.org/10.1007/s00705-016-2935-3.

Melyan, G., Sahakyan, A., Harutyunyan, A., 2015. Micropropagation of grapevine (Vitis vinifera L.) seedless cultivar "Parvana" through lateral bud development. Vitis - J. Grapevine Res. 54, 253–255.

Messmer, N., Bohnert, P., Askani, L., Schumacher, S., Voegele, R.T., Fuchs, R., 2023. Occurrence and distribution of Grapevine pinot gris virus and other grapevine viruses in German viticultural regions. J. Plant Dis. Prot. 130, 1385–1399. https://doi.org/10.1007/s41348-023-00776-y.

Ohana-Levi, N., Cohen, Y., Munitz, S., Michaelovsky, R., Ferman Mintz, D., Hagag, N., Getz, Y., Netzer, Y., 2024. The response of yield, number of clusters, and cluster weight to meteorological factors and irrigation practices in grapevines: a multi-experiment study. Sci. Hortic. (Amsterdam) 326, 112761. https://doi.org/10.1016/j.scienta.2023.112761.

Park, J.W., Faure-Rabasse, S., Robinson, M.A., Desvoyes, B., Scholthof, H.B., 2004. The multifunctional plant viral suppressor of gene silencing P19 interacts with itself and an RNA binding host protein. Virology 323, 49–58. https://doi.org/10.1016/j.virol.2004.02.008.

Prudhomme, N., Pastora, R., Thomson, S., Zheng, E., Sproule, A., Krieger, J.R., Murphy, J.P., Overy, D.P., Cossar, D., McLean, M.D., Geddes-McAlister, J., 2024. Bacterial growth-mediated systems remodelling of Nicotiana benthamiana defines unique signatures of target protein production in molecular pharming. Plant Biotechnol. J. 22, 2248–2266. https://doi.org/10.1111/pbi.14342.

Saldarelli, P., Giampetruzzi, A., Morelli, M., Malossini, U., Pirolo, C., Bianchedi, P., Gualandri, V., 2015. Genetic variability of Grapevine Pinot gris virus and its association with Grapevine leaf mottling and deformation. Phytopathology 105, 555–563. https://doi.org/10.1094/PHYTO-09-14-0241-R.

Saldarelli, P., Gualandri, V., Malossini, U., Glasa, M., 2017. Grapevine pinot gris virus. In: Grapevine Viruses: Molecular Biology, Diagnostics and Management. Springer International Publishing, pp. 351–363. https://doi.org/10.1007/978-3-319-57706-7_17.

Shabanian, M., Li, C., Ebadi, A., Dolja, V., Meng, B., 2023. Optimization of a protocol for launching grapevine infection with the biologically active cDNA clones of a virus. Pathogens 12. https://doi.org/10.3390/pathogens12111314.

Song, Y., Hanner, R.H., Meng, B., 2021. Genome-wide screening of novel RT-qPCR reference genes for study of GLRaV-3 infection in wine grapes and refinement of an RNA isolation protocol for grape berries. Plant Methods 17, 1–20. https://doi.org/10.1186/s13007-021-00808-4.

Tamura, K., Stecher, G., Kumar, S., 2021. MEGA11: molecular evolutionary genetics analysis version 11. Mol. Biol. Evol. 38, 3022–3027. https://doi.org/10.1093/molbev/msab120.

Tarquini, G., Ermacora, P., Bianchi, G.L., De Amicis, F., Pagliari, L., Martini, M., Loschi, A., Saldarelli, P., Loi, N., Musetti, R., 2018. Localization and subcellular association of Grapevine Pinot Gris Virus in grapevine leaf tissues. Protoplasma 255, 923–935. https://doi.org/10.1007/s00709-017-1198-5.

Tarquini, G., Ermacora, P., Firrao, G., 2021a. Polymorphisms at the 3'end of the movement protein (MP) gene of grapevine Pinot gris virus (GPGV) affect virus titre and small interfering RNA accumulation in GLMD disease. Virus Res. 302, 198482. https://doi.org/10.1016/j.virusres.2021.198482.

Tarquini, G., Ermacora, P., Martini, M., Firrao, G., 2023. The conundrum of the connection of grapevine Pinot gris virus with the grapevine leaf mottling and deformation syndrome. Plant Pathol. https://doi.org/10.1111/ppa.13667.

Tarquini, G., Pagliari, L., Ermacora, P., Musetti, R., Firrao, G., 2021b. Trigger and suppression of antiviral defenses by Grapevine Pinot Gris Virus (GPGV): novel insights into virus-host interaction. Mol. Plant Microbe Interact. 34. https://doi.org/10.1094/MPMI-04-21-0078-R.

Tarquini, G., Zaina, G., Ermacora, P., De Amicis, F., Franco-Orozco, B., Loi, N., Martini, M., Bianchi, G.L., Pagliari, L., Firrao, G., de Paoli, E., Musetti, R., 2019. Agroinoculation of grapevine pinot gris virus in tobacco and grapevine provides insights on viral pathogenesis. PLoS One 14, 1–15. https://doi.org/10.1371/journal.pone.0214010.

van den Born, E., Omelchenko, M.V., Bekkelund, A., Leihne, V., Koonin, E.V., Dolja, V.V., Ø Falnes, P., 2008. Viral AlkB proteins repair RNA damage by oxidative demethylation. Nucleic Acids Res. 36, 5451–5461. https://doi.org/10.1093/nar/gkn519.

Várallyay, É., Oláh, E., Havelda, Z., 2014. Independent parallel functions of p19 plant viral suppressor of RNA silencing required for effective suppressor activity. Nucleic Acids Res. 42, 599–608. https://doi.org/10.1093/nar/gkt846.

Vu, M., Vemulapati, B.M., McFadden-Smith, W., Fall, M.L., Úrbez-Torres, J.R., Moreau, D.L., Poojari, S., 2023. Phylogenetic and evolutionary studies of grapevine pinot gris virus isolates from Canada. Viruses 15. https://doi.org/10.3390/v15030735.

Weigel, D., Glazebrook, J.J.C.P., 2006. Transformation of agrobacterium using the freeze-thaw method. CSH Protoc 7, pdb–prot4666.

Xia, Y., Xun, L., 2017. Revised mechanism and improved efficiency of the quikchange site-directed mutagenesis method. Methods Mol. Biol. 1498, 367–374. https://doi.org/10.1007/978-1-4939-6472-7_25.

Xiao, H., Kim, W.S., Meng, B., 2015. A highly effective and versatile technology for the isolation of RNAs from grapevines and other woody perennials for use in virus diagnostics. Virol. J. 12, 1–15. https://doi.org/10.1186/s12985-015-0376-3.

Xiao, H., Li, C., Rwahnih, M. Al, Dolja, V., Meng, B., 2019. Metagenomic analysis of riesling grapevine reveals a complex virome including two new and divergent variants of grapevine leafroll-associated virus 3. Plant Dis. 103, 1275–1285. https://doi.org/10.1094/PDIS-09-18-1503-RE.

Xiao, H., Shabanian, M., Moore, C., Li, C., Meng, B., 2018. Survey for major viruses in commercial Vitis vinifera wine grapes in Ontario. Virol. J. 15. https://doi.org/10.1186/s12985-018-1036-1.

Further reading

Aravind, L., Koonin, E.V., 2001. The DNA-repair protein AlkB, EGL-9, and leprecan define new families of 2-oxoglutarate- and iron-dependent dioxygenases. Genome Biol 2, 1–8. https://doi.org/10.1186/gb-2001-2-3-research0007.

Felsenstein, J., 1985. Confidence limits of phylogeneies: an approach using the bootstrap. Evolution (N. Y). 39, 783–791.

Meng, B., Venkataraman, S., Li, C., Wang, W., Dayan-Glick, C., Mawassi, M., 2013. Construction and biological activities of the first infectious cDNA clones of the genus Foveavirus. Virology 435, 453–462. https://doi.org/10.1016/j.virol.2012.09.045.

Messmer, N., Bohnert, P., Askani, L., Schumacher, S., Voegele, R.T., Fuchs, R., 2024. Grapevine Pinot gris virus spreads in infected vineyards: latent infections have no direct impact on grape production. Virol J 21 (1), 178. https://doi.org/10.1186/s12985-024-02453-4.

Moore, C., Meng, B., 2019. Prediction of the molecular boundary and functionality of novel viral AlkB domains using homology modelling and principal component analysis. J. Gen. Virol. 100, 691–703. https://doi.org/10.1099/jgv.0.001237.

Xiang, C., Han, P., Lutziger, I., Wang, K., Oliver, D.J., 1999. A mini binary vector series for plant transformation. Plant Mol. Biol. 40, 711–717.

Xiao, H., Meng, B., 2023. Molecular and metagenomic analyses reveal high prevalence and complexity of viral infections in French-American hybrids and North American grapes. Viruses (15). https://doi.org/10.3390/v15091949.

Holton, T.A., Graham, M.W., 1991. A simple and efficient method for direct cloning of PCR products using ddT-tailed vectors. Nucleic Acids Res. 19, 1156. https://doi.org/10.1093/nar/19.5.1156.